LBNL-40209
UC-401
Preprint

ERNEST ORLANDO LAWRENCE BERKELEY NATIONAL LABORATORY

Interactions of Lysozyme in Concentrated Electrolyte Solutions from Dynamic-Light-Scattering Measurements

Daniel E. Kuehner, Christiane Heyer,
Christian Rämsch, Ursula M. Fornfeld,
Harvey W. Blanch, and John M. Prausnitz
Chemical Sciences Division

April 1997
Submitted to
Biophysical Journal

REFERENCE COPY
Does Not
Circulate
Bldg. 50 Library - Ref.
Lawrence Berkeley National Laboratory
LBNL-40209
Copy 1

DISCLAIMER

This document was prepared as an account of work sponsored by the United States Government. While this document is believed to contain correct information, neither the United States Government nor any agency thereof, nor The Regents of the University of California, nor any of their employees, makes any warranty, express or implied, or assumes any legal responsibility for the accuracy, completeness, or usefulness of any information, apparatus, product, or process disclosed, or represents that its use would not infringe privately owned rights. Reference herein to any specific commercial product, process, or service by its trade name, trademark, manufacturer, or otherwise, does not necessarily constitute or imply its endorsement, recommendation, or favoring by the United States Government or any agency thereof, or The Regents of the University of California. The views and opinions of authors expressed herein do not necessarily state or reflect those of the United States Government or any agency thereof, or The Regents of the University of California.

Ernest Orlando Lawrence Berkeley National Laboratory
is an equal opportunity employer.

DISCLAIMER

This document was prepared as an account of work sponsored by the United States Government. While this document is believed to contain correct information, neither the United States Government nor any agency thereof, nor the Regents of the University of California, nor any of their employees, makes any warranty, express or implied, or assumes any legal responsibility for the accuracy, completeness, or usefulness of any information, apparatus, product, or process disclosed, or represents that its use would not infringe privately owned rights. Reference herein to any specific commercial product, process, or service by its trade name, trademark, manufacturer, or otherwise, does not necessarily constitute or imply its endorsement, recommendation, or favoring by the United States Government or any agency thereof, or the Regents of the University of California. The views and opinions of authors expressed herein do not necessarily state or reflect those of the United States Government or any agency thereof or the Regents of the University of California.

LBNL-40209
UC-401

Interactions of Lysozyme in Concentrated Electrolyte Solutions from Dynamic-Light-Scattering Measurements

Daniel E. Kuehner, Christiane Heyer, Christian Rämsch, Ursula M. Fornfeld, Harvey W. Blanch and John M. Prausnitz

Department of Chemical Engineering

University of California, Berkeley

and

Chemical Sciences Division

Lawrence Berkeley National Laboratory

Berkeley, CA 94720, USA

This work was supported by the Director, Office of Energy Research, Office of Basic Energy Sciences, Chemical Sciences Division of the U.S. Department of Energy under Contract Number DE-AC03-76SF00098.

Interactions of Lysozyme in Concentrated Electrolyte Solutions from Dynamic-Light-Scattering Measurements

Daniel E. Kuehner, Christiane Heyer[1], Christian Rämsch[2], Ursula M. Fornefeld[3], Harvey W. Blanch* and John M. Prausnitz*

Department of Chemical Engineering
University of California, Berkeley

and

Chemical Sciences Division,
Lawrence Berkeley National Laboratory,
Berkeley, CA 94720

Keywords: potential of mean force, dynamic Zimm plot, ion-osmotic attraction, aggregation

---

[1] Present address: Institut für Verfahrenstechnik, Technical University, Munich

[2] Present address: Institut für Enzymtechnologie, University of Düsseldorf, KFA-Jülich

[3] Present address: Institut für Thermo und Fluiddynamik, University of Bochum

* Authors to whom correspondence should be addressed.

Abstract

The diffusion of hen-egg-white lysozyme has been studied by dynamic light scattering in aqueous solutions of ammonium sulfate as a function of protein concentration to 30 g/L. Experiments were conducted under the following conditions: pH 4-7 and ionic strength 0.05 to 5.0 M. Diffusivity data at pH 4 were interpreted in the context of a two-body interaction model. From this analysis, two potential-of-mean-force parameters, the effective monomer charge and Hamaker constant, were obtained. For pHs greater than 4, the data were analyzed using a model that describes the diffusion coefficient of a polydisperse system of interacting protein aggregates in terms of an isodesmic, indefinite aggregation equilibrium constant. Data analysis incorporated multicomponent virial and hydrodynamic effects. The resulting size distributions indicate only the presence of small lysozyme aggregates over the range of conditions studied.

Introduction

Protein precipitation and crystallization are key steps in the recovery and characterization of virtually all proteins. In industry, salt-induced protein precipitation is frequently used as a first-pass purification step (Scopes, 1994; Rothstein, 1994) while in research, large, high-quality crystals are required for structure determination and studies of structure-function relationships. For these applications, predictive models based on fundamental protein properties would be of considerable benefit. Since precipitation and

crystallization are both aggregation processes driven by intermolecular interactions, it is crucial to understand how equilibrium interactions depend on experimental variables (*e.g.*, protein concentration and purity, salt identity, ionic strength, pH and temperature). Recent work in this area has focused on correlating precipitation and crystallization data with molecular quantities such as the potential of mean force (Tavares and Sandler, 1997; Rosenbaum et al., 1996; Chiew et al., 1995; Mahadevan and Hall, 1992; Vlachy et al., 1993) and the osmotic second virial coefficient (George and Wilson, 1994).

Hen-egg-white lysozyme is a robust, compact globular protein soluble over a broad range of conditions. It is available at high purity and has been studied extensively, making it suitable for investigation of protein-solution behavior. Previous equilibrium-sedimentation experiments have shown that at low concentrations, hen-egg-white lysozyme undergoes a reversible pH-dependent aggregation in solutions of low ionic strength (Sophianopoulos and Van Holde, 1964, 1961). At pH below 4.5, lysozyme is monomeric, while at higher pH, increasing aggregation is observed. This aggregation follows from an attractive interaction between Glu-35 in the active site (Glu-35 has an unusually high $pK_a \approx 6.3$) and Trp-62, with equilibrium aggregates growing in a "head-to-tail" chain-like structure (Norton and Allerhand, 1977; Banerjee et al., 1975; Sophianopoulos, 1969; Blake et al., 1967; Rupley et al., 1967). Other equilibrium studies of lysozyme aggregation at higher (but undersaturated) concentrations have been interpreted using either monomer-dimer equilibria or models with higher aggregates (Deonier and Williams, 1970; Adams and Filmer, 1966; Bruzzesi et al., 1965). Wills *et al.* (1980) performed ultracentrifugation experiments with lysozyme at concentrations to 60

mg/mL at pH 8.0; they analyzed their data in the context of an indefinite isodesmic association, concluding that aggregates up to decamers contributed significantly.

Many experimental investigations of lysozyme aggregation have been reported in the protein-crystallization literature in the last decade, both for supersaturated and undersaturated solutions in typical crystallizing solvents (*e.g.*, 2-4% sodium chloride by weight, acetate-buffered at pH 4.2 - 4.6). It remains an open question whether lysozyme forms large aggregates when undersaturated or when in the prenucleation phase of crystallization. Recent data which support aggregation are from small-angle neutron scattering (SANS) experiments (Niimura et al., 1995a,b, 1994; Boué et al., 1993) and dialysis kinetics (Wang, 1996; Wilson, 1996, 1993). In contrast, some dynamic-light-scattering (DLS) studies have concluded that scattering data that may at first examination suggest the formation of aggregations, are more accurately explained in terms of interparticle interactions (Muschol and Rosenberger, 1996, 1995; Eberstein et al., 1994). DLS is a powerful tool for investigating intermolecular interactions and aggregation of proteins over a broad range of solution conditions (Shen et al., 1995; Thibault et al., 1992; Skouri et al., 1992, 1991; Murphy et al., 1991; Mikol et al., 1990). We report here the results of DLS measurements at 25°C for hen-egg-white lysozyme at concentrations to 30 g/L in solutions of the commonly-used precipitating salt ammonium sulfate. To examine the regime where aggregation has been reported, pH ranged from 4 to 7. Ionic strength varied between dilute and near-salting-out conditions (0.05 - 5.0 M). Solutions of high ionic strength were studied to obtain insight on interactions between proteins at solution conditions near precipitation or crystallization. DLS data at pH 4 were interpreted in the

context of a model that relates the measured diffusion coefficients to a two-body potential of mean force between proteins. From this analysis, two molecular interaction parameters, the protein effective charge and Hamaker constant, are obtained for the monomer. At higher pH, the model was generalized to account for aggregation by introducing an indefinite isodesmic association reaction, with a corresponding multicomponent diffusion model for polydisperse systems of interacting particles (Batchelor, 1983, 1982, 1976). From this model, effective equilibrium aggregation constants were found to be small under all solution conditions investigated, indicating that lysozyme does not aggregate significantly, even when salt concentration approaches protein-precipitation conditions (Coen et al., 1995).

Materials and Methods

Lysozyme Purification

Two grades of hen-egg-white lysozyme were obtained from Sigma (St. Louis, MO) and stored dessicated at -5°C. The first (L-2879; Lot 15H7090, CAS [52219-07-5]) was lysozyme chloride, three-times crystallized (neither dialyzed nor lyophilized), containing approximately 90% protein by weight, with the remainder as sodium acetate and sodium chloride. The enzymatic activity of this grade was 65,000 units/mg. The second grade (L-6876; Lots 111H7010 and 53H7145, CAS [12650-88-3]) contained lysozyme, three-times crystallized, dialyzed and lyophilized, approximately 95% protein by

weight, with the remainder sodium acetate and sodium chloride, and specific activity of 50,000 units/mg. For the experiments with ionic strength to 1.0 M, lysozyme L-2879 was purified by size-exclusion chromatography at pH 3 (HCl) in a 5 x 60-cm column packed with Toyopearl HW50-F (Supelco, Bellefonte, PA). The central portion of the lysozyme peak was collected, concentrated to 30 mg/ml protein via ultrafiltration, and exhaustively dialyzed against ammonium-sulfate solutions of the desired ionic strength. DLS samples with lower protein concentrations were prepared by dilution with an ammonium-sulfate solution of the same ionic strength, and pH adjusted with small volumes of conjugate acid or base. All solutions were loaded into DLS sample cells within a few hours of preparation. In the experiments with ionic strength between 3.0 and 5.0 M, lysozyme L-6876 was used as supplied, without further purification.

A.C.S.-grade ammonium sulfate (CAS [7783-20-2]), sulfuric acid (CAS [7664-93-9]) and ammonium hydroxide (CAS [1336-21-6]) were obtained from Fisher Scientific. Distilled, deionized and 0.2-μm-filtered water was dispensed from a Barnstead NANOpure system.

Dynamic-Light-Scattering Measurements

The dynamic-light-scattering system consisted of an Innova-90 argon-ion laser (Coherent, Inc., Santa Clara, CA) vertically polarized, tuned to 488 nm and operating at output power between 50-500 mW, a BI-240SM multi-angle goniometer, a BI-EMI-9865 photomultiplier and a BI-9000 digital autocorrelator (Brookhaven Instruments Corp.,

Holtsville, NY). The BI-9000 is capable of calculating in real time the electric-field autocorrelation function, $g^E(\tau)$, that yields z-average diffusion coefficients, $\overline{D}$. Decalin ($C_{10}H_{18}$, Aldrich 29477-2, CAS [91-17-8], refractive index $n \approx 1.47$) was used as an index-matching liquid to reduce flare. Sample temperature was maintained at 25°C (±0.2°C) with a VWR Model 1160 recirculating water bath. Sample cells were precision-ground Pyrex NMR tubes with 12-mm O.D., 0.5-mm wall thickness and $n = 1.49$ (Wilmad Glass, Buena, NJ), with a volume of 5 mL. After cleaning, loading and sealing the sample tubes in a low-dust environment, samples were recirculated through an in-line membrane filter cartridge, using a peristaltic pump, until a dust-free trial autocorrelation function was observed at $\theta = 30°$. Filtration times ranged from 10-90 minutes, and the necessary filter pore size varied: 0.2-μm Millex-GV (Millipore, Bedford, MA), 0.1-μm Millex-VV, or Anotop 0.02-μm (Whatman, Clifton, NJ). UV spectrophotometric assays showed that at the end of each experiment, protein loss due to filtration was less than 5% in all cases. Filtration flows were approximately 2 mL/minute to avoid shear-induced protein denaturation. Subsequent to filtration, the samples were allowed to equilibrate for at least 30 minutes before data acquisition commenced. At the same time, the index-matching fluid was recirculated through a 47-mm O.D. 0.1-μm pore-size hydrophobic membrane filter (GSEP 047A0, Millipore) until visual inspection indicated dust-free decalin. All components in the decalin-filtration system consisted of solvent-resistant materials: Teflon and Viton tubing, a magnetically-coupled gear-pump head with stainless-steel and Teflon internals, a stainless-steel filter housing, and a quartz index-matching vessel.

In a typical experiment, the scattered-light intensity was measured from 30° to 90°

in ten-degree increments. For each sample, three measurements were made at each angle. Data were collected over a period of ten to thirty minutes, depending on the angle and the protein concentration, with a minimum photon count of $5 \cdot 10^8$. Data were rejected if the difference between calculated and measured baselines of the autocorrelation function was greater than 0.02%. The majority of accepted data had baseline agreement of $\approx$ 0.01%.

To obtain diffusion coefficients from autocorrelation data, the quadratic cumulant expansion analysis was employed (Koppel, 1972). In most cases, the second central moment of the diffusion-coefficient distribution, Q, was small (<0.02), indicating narrow size distributions. For the few cases where Q was greater than 0.02, inversion of the autocorrelation function was performed with Brookhaven Instruments Corporation's version of the CONTIN program (Provencher, 1982a,b). BI-CONTIN results routinely indicated narrow unimodal diffusion-coefficient distributions centered near the value of $\overline{D}$ given by the quadratic cumulant result. Salt-scattering effects were eliminated by discarding the first few autocorrelator channels when performing distribution analyses. The data were time-independent over the course of a run, typically about five hours. Frequent checks were made by repeating the measurements at $\theta = 30°$ after completing measurements at $\theta = 90°$; no significant differences were observed, indicating that the samples were in a stationary state over the time scale of these experiments. Protein concentrations were sufficiently low that multiple-scattering effects were not considered.

At the conclusion of each DLS experiment, protein concentrations were determined by measuring absorbance at 280nm and 25°C using a Beckman DU-6

spectrophotometer. The extinction coefficient used for lysozyme was 2.635 L/(g-cm) (Sophianopoulos and Van Holde, 1964). The refractive index of each sample was measured with a Zeiss refractometer using white light. Refractive indices increased linearly with lysozyme concentration; the observed refractive-index increment, $(dn/dc)_{T,p}$ was 0.18 mL/g, a typical value for most proteins.

Experimental Results

Light-scattering experiments were conducted over the pH range 4 to 7, with ammonium sulfate ionic strength between 0.05 and 5.0 M and lysozyme concentration between 5 and 30 mg/mL. At each pH and ionic strength, three protein concentrations were examined over the angular range 30° to 90°. Figure 1 shows a typical dynamic Zimm plot (Stepanek, 1993) where, for a given pH and ionic strength, the average apparent diffusion coefficient $\overline{D}$ (in cm^2/sec), obtained from DLS autocorrelation data is plotted for each protein concentration as a function of an angular parameter, $q^2 + kc_p$, where c_p is the total molar concentration of protein. The extrapolated value of $\overline{D}$ is the infinite-dilution zero-angle self-diffusion coefficient, D_0, corresponding to the diffusion of an isolated monomer. Diffusion-coefficient data are compiled in Table 1. In Figure 1, as in all experiments, the measured $\overline{D}$'s show little dependence on the magnitude of the scattering vector, q, suggesting that samples in these experiments contained narrow unimodal distributions of small oligomers.

Infinite-Dilution Diffusivities

Figure 2 shows infinite-dilution hydrodynamic radii, r_0 (in Å), obtained from dynamic Zimm plots via the Stokes-Einstein equation for infinitely-dilute monodisperse spheres:

$$D_0 = \frac{k_B T}{f_0} = \frac{k_B T}{6\pi\eta_0 r_0} \cdot 10^{17} \qquad (1)$$

where f_0 is the hydrodynamic friction factor, k_B is Boltzmann's constant, T is absolute temperature, and η_0 is the viscosity of the solvent (in centipoise). Values for η_0 as a function of ammonium sulfate ionic strength at 20°C were taken from the literature (Weast, 1981) and corrected for temperature.

At pH 4, the average value for r_0 is 18 Å (±0.5 Å), in good agreement with DLS measurements reported previously for lysozyme at low pH in various salt solutions by Nicoli and Benedek (1976), who calculated from DLS measurements a hydrodynamic radius of 18.5 Å over a pH range of 1.2 to 2.3 in solutions of 0.2 M potassium chloride, where lysozyme is entirely monomeric. Mikol and coworkers (1990) determined the hydrodynamic radius of lysozyme to be 19.1 Å in solutions of ammonium sulfate at ionic strengths between 6 and 9 M, buffered to pH 4.6 with 40 mM sodium acetate. Eberstein *et al.* (1994) reported a radius of 20.9 Å in solutions of 0.1 M sodium acetate buffered to

pH 4.2, with additional sodium chloride concentrations up to 1.4 M. Muschol and Rosenberger (1995) found a radius of 19 Å for lysozyme in solutions of sodium chloride and acetate at pH 4.7, with total salt concentrations to 0.5 M. Skouri and coworkers (1992) reported r_0 = 22 Å in solutions of sodium chloride, buffered to pH 4.6 with 40 mM sodium acetate, over the temperature range 13 - 22°C. The differences in the above-mentioned literature values for the hydrodynamic radius may reflect differences in experimental technique and the use of different salts and ionic strengths in each of those studies. Protein-concentration effects may also be reflected in those data because the radii reported were not all obtained from infinite-dilution diffusivities. Further, other protein impurities may have been present in the lysozyme used in those experiments.

Lysozyme hydrodynamic radii obtained from DLS are slightly larger than the equivalent spherical radius, r_x, of the unhydrated lysozyme monomer, as determined by X-ray crystallography at pH near 4. The crystal structure of hen-egg-white lysozyme (Brookhaven protein database structure 2LYZ) shows that the unhydrated monomer is a prolate ellipsoid of revolution with major semiaxis α_x = 22.5 Å and symmetric minor semiaxes β_x = 15 Å, corresponding to r_x = 17.2 Å. Surrounding the lysozyme molecule are bound water molecules that diffuse with the protein in solution; these bound water molecules are therefore reflected in the diffusivities measured by DLS. Close to the surface of the protein are salt ions that may either bind tightly due to specific salt-protein interactions (within the Stern layer) or associate within the Gouy-Chapman layer to reduce the protein net charge. These ions also affect the measured diffusivities. While the extrapolation of the dynamic Zimm plot yields D_0 values which reflect the absence of

protein-protein interactions, specific salt-protein (ion-binding) and water-protein (hydration) effects remain. In general, for a given protein these interactions depend strongly on the identity and ionic strength of the salt and to a lesser degree on pH (Arakawa and Timasheff, 1982; Melander and Horvath, 1977). The difference between the hydrodynamic radius reported at pH 4 and the unhydrated radius is defined here as $r_0 - r_x = \Delta r$; it is assumed to account for hydration and ions within the Stern layer and is further assumed to be constant over the ranges of ionic strength and pH investigated. For the data shown in Figure 2, Δr = 0.8 Å. The values of r_0 show no clear dependence on ionic strength, indicating qualitatively that salt-protein interactions do not change significantly within the range of salt concentrations investigated. Similarly, no effect of pH on the infinite-dilution data was observed, confirming that the extrapolated values are truly free of protein-protein interaction effects.

Concentration-Dependent Diffusivities

Figure 3 illustrates the dependence of the normalized average apparent diffusion coefficient, $\overline{D}/D_0$, on protein concentration and pH for several values of ionic strength and pH. Here, the $\overline{D}$ at each protein concentration is the zero-angle extrapolated value. Protein concentration is expressed as volume fraction, given by $\phi = c_p M \bar{v}/1000$, where M is the molecular weight (14,600 g/mol) and $\bar{v}$ is the partial specific volume of lysozyme, 0.703 mL/g (Sophianopoulos et al., 1962). In all experiments reported here, a linear relationship is observed between $\overline{D}/D_0$ and ϕ, with a slope that varies with solution

pH and ionic strength. The slope, λ, contains information about interactions between proteins; for monodisperse (i.e., non-aggregating) systems, a formal relationship between λ and the potential of mean force (PMF) is available (Batchelor, 1983, 1982, 1976; Felderhof, 1978, 1977). For repulsive interactions, λ is positive, while for strong attractive interactions, λ is negative.

As shown in Figure 3(*a*), λ decreases with increasing ionic strength at pH 4, first making a transition from positive to negative between 0.05 M and 0.15 M, then plateauing at 0.5 M, then exhibiting a further decrease for ionic strength greater than 1.0 M. Similar dependence of λ on ionic strength was observed for pH 5 - 7. Figure 3(*b*) shows that λ also depends strongly on pH at low ionic strength. However, as ionic strength increases, this dependence is gradually lost [see Figure 3(*c*)]. The data in Figure 3 for ionic strength indicate that a shift occurs in the balance of interactions between lysozyme monomers, from repulsive at low pH and low ionic strength toward greater attraction as either pH or ionic strength (or both) increase.

The plateau in λ with increasing ionic strength shown in Figure 3(*a*) can be readily attributed to screening of Coulombic repulsion between proteins, as described in detail in the following section. However, the further decrease in λ as ionic strength exceeds 1.0 M suggests the presence of other ionic-strength-dependent interaction(s) which contribute significantly at higher salt concentrations. The decrease in λ could also indicate aggregation of lysozyme; for solutions of such high ionic strength, approaching the salt concentration where protein precipitation is induced, one might expect to observe large

equilibrium clusters of protein molecules. However, for aggregating solutions, the dependence of $\overline{D}/D_0$ on protein concentration is not linear, due to the presence of particles of different sizes. Therefore, the linear nature of the data for ionic strength greater than 1.0 M suggests that significant aggregation does not occur in these solutions.

Discussion

The Potential of Mean Force (PMF)

Protein interactions can be described quantitatively by a two-body potential of mean force; three-body and higher interactions become important at protein concentrations higher than those reported here. Selection of the proper form of the potential of mean force requires knowledge of the dominant physical interactions between protein in equilibrium solutions. In low-ionic-strength solutions, proteins interact primarily through a balance of coulombic repulsion and attractive dispersion forces that can be described by the DLVO theory (Verwey and Overbeek, 1948). However, in high-ionic-strength solutions where salt-induced protein precipitation occurs, macromolecular coulombic interactions are essentially screened and the overall interaction is attractive. Furthermore, because little free water for solvation remains available to the protein, osmotic effects become significant. The following multicomponent potential-of-mean-force model accounts for all these phenomena in aggregating lysozyme solutions. A one-component form has been used previously to describe osmotic-pressure data (Vlachy et

al., 1993) and precipitation phase-equilibrium results (Tavares and Sandler, 1997); a similar form is applied here to obtain from DLS data at pH 4 two potential parameters specific for lysozyme. The multicomponent form is used to estimate aggregate-size distributions from the high-ionic-strength data, as described below.

For simplicity in PMF modeling, lysozyme monomers and oligomers are considered effective spheres. The centrosymmetric potential of mean force between an *i*-mer and a *j*-mer, $W_{ij}(r)$, is considered here to be the sum of four contributions:

$$W_{ij}(r) = W_{ij}^{HS}(r) + W_{ij}^{elec}(r) + W_{ij}^{disp}(r) + W_{ij}^{osm}(r) \qquad (2)$$

The hard-sphere potential, $W_{ij}^{HS}(r)$, is:

$$W_{ij}^{HS}(r) = \begin{cases} \infty & r \le \sigma'_{ij} \\ 0 & r > \sigma'_{ij} \end{cases} \qquad (3)$$

where $\sigma'_{ij} = (\sigma'_i + \sigma'_j)/2$; σ'_i and σ'_j are the hydrated effective hard-sphere diameters of oligomers *i* and *j*, *i.e.*, $\sigma_i + 2\Delta r$ and $\sigma_j + 2\Delta r$. The effective hard-sphere diameters for protein aggregates are estimated by considering the "head-to-tail" nature of the lysozyme aggregation, described earlier, and the crystal structure of lysozyme. Aggregates were considered to have a simplified effective ellipsoidal geometry, shown in Figure 4, with hydrated major and minor semiaxes α'_i and β', respectively. For an aggregate thus

described as a rigid prolate ellipsoid of revolution, the hydrodynamic friction factor, f_i, is given by (Zero and Pecora, 1985):

$$f_i = 6\pi\eta_0\alpha_i \frac{\left(1-\rho_i^2\right)^{0.5}}{\ln\left\{\left[1+\left(1-\rho_i^2\right)^{0.5}\right]/\rho_i\right\}} \tag{4}$$

where $\rho_i = \beta'/\alpha_i'$. Equating this friction factor with that of the equivalent hydrated effective sphere, $3\pi\eta_0\sigma_i'$, with the assumption of non-interpenetrating hydration/Stern layers of thickness Δr, yields the unhydrated aggregate effective hard-sphere diameter, σ_i. The ellipsoidal aggregate hydrated semiaxes are defined as $\alpha_i' = i\cdot\alpha_x + \varepsilon$ and $\beta' = \beta_x + \varepsilon$, where ε is the thickness of the hydration/Stern layer around the aggregate; ε is estimated from infinite-dilution data at pH 4 by equating the ellipsoidal friction factor for a hydrated monomer, *i.e.* f_1, with that of the corresponding effective spherical monomer, $6\pi\eta_0\left(r_x + \Delta r\right)$. For Δr = 0.8 Å, ε = 0.6 Å and is assumed to be constant over the ranges of ionic strength and pH investigated. This method is reasonable for small rigid linear aggregates; for large aggregates, a wormlike-chain or rod model for the friction factor would be more appropriate.

The repulsive screened coulombic interaction, $W_{ij}^{elec}(r)$, is given in the mean-field approximation by (Verwey and Overbeek, 1948):

$$W_{ij}^{elec}(r) = \frac{z_i z_j e^2 \exp\left[-\kappa(r-\sigma_{ij})\right]}{4\pi\varepsilon_0\varepsilon_r \cdot r \cdot (1+\kappa\sigma_i)(1+\kappa\sigma_j)} \qquad r \geq \sigma'_{ij} \tag{5}$$

where z_i is the pH-dependent valence of the i-mer, e is the unit charge, and κ is the Debye screening parameter, given by $\kappa^2 = (2e^2 N_A I)/(k_B T \varepsilon_0 \varepsilon_r)$; ε_0 is the dielectric permittivity of the vacuum, ε_r is the dielectric constant, and N_A is Avogadro's number. The ionic strength due to added electrolyte is given by $I = 0.5 \cdot \sum c_m z_m^2$, where c_m and z_m are the molar concentration and valence of ion m, respectively. The protein and its counterions are neglected in calculating the ionic strength. The protein monomer valence, z_1, is a parameter of the model regressed from the low-pH data, as described later. Because the isoelectric point of lysozyme is 11.1, the protein has a positive charge at all conditions studied here.

The unretarded attractive dispersion potential, $W_{ij}^{elec}(r)$, for spherical particles (Hamaker, 1937), for $r \geq \sigma'_{ij}$, is:

$$W_{ij}^{disp}(r) = -\frac{H}{12}\left\{\frac{\sigma_i\sigma_j}{r^2-\sigma_{ij}^2} + \frac{\sigma_i\sigma_j}{r^2-(\sigma_i-\sigma_j)^2/4} + 2\cdot\ln\left[\frac{r^2-\sigma_{ij}^2}{r^2-(\sigma_i-\sigma_j)^2/4}\right]\right\} \tag{6}$$

where H is the Hamaker constant for the interaction between the i-j pair. Since H is primarily a function of the chemical composition of the protein molecules, the Hamaker constant is assumed to be the same for all protein aggregates in solution. Further, the

Hamaker constant is expected to decrease only slightly due to dielectric screening as the ionic strength increases to 5.0 M (Israelachvili, 1992). Equation 6 diverges in the limit of particle contact, *i.e.* $r = \sigma_{ij}$. Hence, the concept of a non-interpenetrating hydration/Stern layer of thickness Δr (obtained from infinite-dilution data) preserves applicability of Equation 6. The effective Hamaker constant is a model parameter and is determined here from low-pH, low-ionic-strength DLS data.

In concentrated electrolyte solutions, ions occupy a significant fraction of the total solution volume. When two protein molecules or aggregates approach contact, ions are excluded from a region between the protein particles. This causes an imbalance in the local osmotic pressure exerted by the ions on the proteins, approximated by the ideal osmotic pressure of the solution, $\Pi_{id} = \rho_s k_B T$, where ρ_s is the total ion number density. The result is a strong short-range attractive potential between the proteins, expressed by (Asakura and Oosawa, 1954; Mahadevan and Hall, 1992):

$$W_{ij}^{osm}(r) = \begin{cases} \dfrac{-2\pi}{3} \cdot \Pi_{id} \cdot (\xi_i^3 + \xi_j^3) \cdot \left[1 - \dfrac{r^3}{8(\xi_i^3 + \xi_j^3)} - \dfrac{3r}{4} \dfrac{(\xi_i^2 + \xi_j^2)}{(\xi_i^3 + \xi_j^3)} - \dfrac{3}{8r} \dfrac{(\xi_i^2 - \xi_j^2)^2}{(\xi_i^3 + \xi_j^3)} \right] & \sigma'_{ij} \le r \le \sigma'_{ij} + \overline{\sigma_{ion}} \\ 0 & r > \sigma'_{ij} + \overline{\sigma_{ion}} \end{cases} \quad (7)$$

The ion-oligomer radius $\xi_i = (\sigma'_i + \overline{\sigma_{ion}})/4$, where $\overline{\sigma_{ion}}$ is the average ion diameter. In this contribution to the overall potential of mean force, the ions are hard spheres; electrostatic effects are taken into account by the repulsive screened coulombic potential.

Figure 5(*a*) illustrates the magnitude of the contributions to the potential of mean force for protein monomers at pH 4 at 0.05 M ionic strength. At 0.05 M ionic strength, coulombic repulsion is strong and there is a significant barrier to aggregation. The salt concentration is sufficiently low that the attractive contribution from ion-osmotic effects is negligible. However, at small separations, the overall potential is attractive due to strong attractive dispersion interaction. Figure 5(*b*) shows the dependence of the overall potential of mean force on ionic strength. As ionic strength increases, the repulsive barrier diminishes due to screening of the repulsive coulombic contribution and increased osmotic attraction. At the highest ionic strength, 5.0 M, attractive osmotic effects contribute significantly when the proteins are near contact. Here, the overall PMF is governed by the dispersion interaction for separations greater than the range of the osmotic-attraction contribution. As noted by George and Wilson (1994), in solutions that precipitate (*e.g.*, high salt concentration), the potential of mean force is strongly attractive.

Regression of PMF Parameters at Low pH and Ionic Strength

All DLS measurements were performed in the long-time, or hydrodynamic, regime, where the time scale of the light-scattering experiment, τ, is much greater than either the intrinsic time scale for Brownian motion or that for direct interparticle interactions (Pusey and Tough, 1985). In this regime, experimental values for $\overline{D}$ may be related quantitatively to interparticle interactions. Theoretical studies by Batchelor (1976) and Felderhof (1978) take into account both direct (virial) interparticle force and

hydrodynamic effects (*e.g.*, Oseen forces). In systems of monodisperse interacting particles, λ is related to the potential of mean force by:

$$\lambda = \int_{\sigma_i'}^{\infty} F(r,\sigma_i') \cdot g_{ii}(r) dr \tag{8}$$

where, in the dilute-protein limit, the pair-correlation function for two particles of type i, $g_{ii}(r)$, is given by:

$$g_{ii}(r) = exp\left(-\frac{W_{ii}(r)}{k_B T}\right) \tag{9}$$

The exact form of the geometric function $F(r,\sigma_i')$ depends on the assumptions made regarding hydrodynamic interactions; the form of $F(r,\sigma_i')$ derived by Batchelor is used in this work.

The potential of mean force outlined above contains two adjustable parameters: the Hamaker constant, H, and the protein monomer valence, z_1; both are obtained from the data at pH 4 where lysozyme is a monomer. For each ionic strength between 0.05 M and 0.5 M, a curve was generated representing the set of $\{H, z_1\}$ points that satisfy the constraint that the experimentally-measured concentration dependence of the diffusion coefficient and the λ calculated from Equation 8 are equal, as shown in Figure 6. The common intersection of these curves for different ionic strengths occurs at $H/k_B T$ = 7.6

and z_1 = 5.3. This procedure has been used previously by several authors, with various forms of the PMF, to obtain molecular-interaction parameters. Corti and Digiorgio (1981) used the DLVO potential of mean force to interpret DLS data in a study of interactions between sodium dodecyl sulfate micelles in solutions of sodium chloride at two ionic strengths. Eberstein *et al.* (1994) studied diffusion of hen-egg-white lysozyme in acetate-buffered (pH = 4.2) solutions of sodium chloride at 25°C and pH 4.2 over the ionic-strength range 0.05 - 1.40 M; they obtained H/k_BT = 7.6 and z_1 = 6.4. More recently, Muschol and Rosenberger (1995) performed static and dynamic-light-scattering measurements on lysozyme in solutions of sodium chloride and sodium acetate at pH 4.7 with total ionic strength from 0.05 to 0.5 M. Using the same expression for the screened coulombic repulsion potential as that used by Eberstein *et al.*, they calculated from DLS data H/k_BT = 7.2 and z_1 = 5.4.

The Hamaker constant for the interaction of two colloidal particles depends primarily on their chemical compositions which determine the magnitude of their overall electronic polarizabilities. It also depends on the dielectric properties of the medium containing the particles. Hence, H depends to some extent on the ionic strength of the protein solution. Further, as solution pH changes, the net fixed proton charge of the protein changes; the effect of this change is taken into account by Equation 5; the very small effects of pH on H are neglected. We estimate the Hamaker constant for the interaction of two lysozyme monomers, based on Lifshitz theory (Israelachvili, 1992) using average protein dielectric properties, to be $H/k_BT \approx 5$ at low ionic strength, with a decrease of approximately 5% at 5.0 M ionic strength due to screening of (weak)

permanent-dipole effects. This result indicates that assuming the dispersion interaction to be independent of ionic strength is reasonable for calculating H from DLS data. Also, this value is in fair agreement with the DLS results presented here and those of other workers cited above. Further, it is consistent with results reported in the literature obtained using other experimental techniques such as membrane osmometry (Haynes, 1992) and low-angle laser-light scattering (Coen et al., 1995; Curtis et al., 1997, *in press*). Other workers have provided estimates of H using more complete descriptions of protein shape and composition. For example, Roth and coworkers (1996) have calculated an effective Hamaker constant for the interaction between bovine serum albumin (BSA) molecules in salt-free water; it is $H/k_BT = 3.10$.

The regressed value of the lysozyme monomer valence, $z_1 = 5.3$, differs significantly from the titration data reported by Tanford and Wagner (1954) who measured a net proton association of +14 at pH 4 for lysozyme in solutions of potassium chloride at 0.15 M ionic strength. However, Riès-Kautt and Ducruix (1994) have shown that lysozyme binds sulfate anions on the surface. The form of the screened coulombic repulsion potential used in this work requires the surface charge of lysozyme which includes both the proton charge and the sum of the charges of the ions in the Stern layer. The loosely bound ions in the diffuse double layer are neglected. Considering the effect of sulfate surface binding, which is assumed to be saturated at 0.05 M ionic strength, the net charge at pH 4 reported here seems reasonable.

Muschol and Rosenberger (1995) have commented on the sensitivity of this

regression method to the value chosen for Δr which determines the lower limit of the PMF integrations in Equation 8. The sensitivity arises from the divergent nature of Equation 6 for the case $\Delta r = 0$, *i.e.* $r = \sigma_{ij}$. Significantly different results are obtained by allowing Δr to vary slightly, as shown in Figure 7. For regressing the Hamaker constant and the monomer valence, and performing subsequent calculations of aggregation equilibrium constants at higher pH's, a physical basis for the choice of Δr is required. The value Δr = 0.8 Å chosen for this work was the average calculated from examining Figure 2 at pH 4 with the assumption that lysozyme is monomeric at this pH. The average was chosen because no systematic variation in r_0 with ionic strength was observed at pH 4.

To verify this, the regressed values of the Hamaker constant and monomer valence (adjusted for pH using experimental titration data for lysozyme) were used to calculate values of λ for pH 5-7 at ionic strengths between 0.05 and 0.5 M.. In all cases the calculated values of λ matched the experimental values within a few percent, indicating the monomer interaction model describes the data well. This is not necessarily a contradiction to the pH-dependent dimerization equilibrium reported for lysozyme (Sophianopoulos and Van Holde, 1964) because it is generally acknowledged that it is not possible to resolve quantitatively monomers from dimers of such small molecules with DLS. However, if significant aggregation were to occur, the monomer model would not describe the normalized-diffusion-coefficient data of Figure 3, and aggregates would be detected by DLS.

A Chemical-Association Model for Lysozyme Aggregation

To quantify aggregation in lysozyme solutions of ionic strength greater than 1.0 M, a nonideal, indefinite, isodesmic association model is applied here. The equilibria are:

$$\begin{aligned} 2L_1 &\xleftrightarrow{K_2} L_2 \\ L_2 + L_1 &\xleftrightarrow{K_3} L_3 \\ L_3 + L_1 &\xleftrightarrow{K_4} L_4 \\ &\ldots etc. \end{aligned} \tag{10}$$

Here, L_1 is the lysozyme monomer, L_2 is the dimer, and so on. The equilibrium constant K_i is defined as:

$$K_i = \frac{a_i}{a_{i-1}a_1} \tag{11}$$

where $a_i = \gamma_i c_i$ is the activity of an i-mer. The standard state is an ideal solution of unit concentration; c_i and γ_i are molar concentration and activity coefficient of an i-mer, respectively. For isodesmic association, K_i is assumed to have the same value for all association steps; hence, the activity of any i-mer is given in terms of the monomer activity, a_1, and the equilibrium constant, K (in L/mol), as follows (Wills et al., 1980):

$$a_i = K^{(i-1)} a_1^i \tag{12}$$

The total molar concentration of protein, c_p, is:

$$c_p = \sum_i i c_i = \sum_i i K^{(i-1)} \frac{a_1^i}{\gamma_i} \tag{13}$$

For dilute and semidilute solutions, the composition-dependent activity coefficient of an *i*-mer, γ_i, is given by:

$$\ln \gamma_i = \sum_j A_{ij} c_j \tag{14}$$

where the summation is for all solute species, including *i*. Parameters A_{ij} (in L/mol) are related to the osmotic second virial coefficients, B_{ij} (also in L/mol), by:

$$A_{ij} = 2B_{ij} - M_j \bar{v}/1000 \tag{15}$$

where M_j is the molecular weight of a *j*-mer. The osmotic second virial coefficient for the interaction between an *i*-mer and a *j*-mer, B_{ij} is related to the potential of mean force through the pair correlation function:

$$B_{ij} = 2\pi N_A \cdot 10^{-27} \cdot \int_0^\infty \left[1 - g_{ij}(r)\right] r^2 dr \tag{16}$$

where N_A is Avogadro's number and r is in Å.

The equilibrium constant, K, can be calculated from protein-diffusion data obtained by DLS experiments. The experimentally-measured quantity is the z-average apparent diffusion coefficient, $\overline{D}$ (Weiner, 1984):

$$\overline{D} = \frac{\sum_i c_i M_i^2 D_i}{\sum_i c_i M_i^2} = \frac{\sum_i M_i^2 K^{(i-1)} \alpha_1^i / \gamma_i \cdot D_i}{\sum_i M_i^2 K^{(i-1)} \alpha_1^i / \gamma_i} \tag{17}$$

where D_i is the diffusivity of the i-mer in solution. For dilute polydisperse systems of interacting spheres, D_i is given by (Batchelor, 1983):

$$D_i = D_{i,0}\left[1 + \Lambda_{ii}\phi_i + \sum_{j \neq i} S_{ij}\phi_j\right] \tag{18}$$

where volume fraction ϕ is given by $c_p \bar{v}/1000$ and the $D_{i,0}$ are the infinite-dilution diffusion coefficients of the i-mers. The $\{\Lambda_{ii}\}$ account for the interactions (virial and hydrodynamic) between aggregates of the same size. The $\{S_{ij}\}$ represent the effects of other aggregate species on the diffusion of an i-mer. These terms also include contributions from both virial and hydrodynamic interactions; they are integral functions of

the multicomponent potential of mean force and the aggregate size ratio, σ_j'/σ_i'. The $D_{i,0}$ are approximated by $D_{i,0} = k_B T/f_i$ where the friction factors, f_i, are given by Equation 4. For a monodisperse solution, $\Lambda_{ii} = \lambda$, all $S_{ij} = 0$, and the one-component model described above is recovered.

The model summarized in Equations 10 - 18 was used to calculate an equilibrium constants, K, from the DLS data for each solution condition (*i.e.*, a given pH and ionic strength), using an iterative technique described in Appendix A. In evaluating the multicomponent potential of mean force, the effective Hamaker constant regressed from the pH-4 data was used at all other pHs and was assumed to have the same value for all aggregates. The monomer valence at pH 4 was adjusted for pH using experimental titration data for lysozyme. For ionic strengths up to 1.0 M, the calculated equilibrium constants were small enough to indicate only traces (essentially negligible) of aggregation, confirming the previous hypothesis made by examination of Figure 3: the diffusion data for ionic strength less than 1.0 M from pH 4 - 7 reflects only the effects of interparticle interactions. For higher ionic strengths, small populations of dimers and trimers are indicated from the calculated size distributions. As noted previously, it is difficult to resolve narrow size distributions of such small particles from DLS data. Hence, the general conclusion is that significant aggregation – for example, the formation of pre-precipitation aggregates, or "praggs" (Mikol et al., 1990) – does not occur for lysozyme at concentrations to 30 g/L in ammonium sulfate solutions of ionic strength to 5.0 M.

The absence of pre-precipitation aggregates is in accord with the studies of Muschol and Rosenberger (1996, 1995) who suggest that many previous scattering studies of lysozyme in crystallization solvents have overestimated protein aggregation by neglecting the effects of attractive intermolecular forces and hydrodynamic interactions. To illustrate further the importance of accounting for solution non-ideality, ideal equilibrium constants were calculated from the DLS data for ionic strength 1.0 M and greater. These equilibrium constants were based on the above aggregation model, but effects of interparticle interactions and molecular excluded volume were not considered. The ideal equilibrium constants were greater than those that included interaction effects, and the values increased significantly with pH and ionic strength. The difference is substantial for solutions of high ionic strength, indicating that osmotic-attraction effects in the potential of mean force make a significant contribution.

Both the screened coulombic-repulsion and dispersion-attraction potentials rely on a mean-field description of the ions as part of a one-component salt/water pseudosolvent. This approximation is acceptable at very low ionic strength but becomes less valid with increasing salt concentration. Applying such an approximate description of electrostatic interactions at ionic strengths greater than 0.1 M is a significant extrapolation. A potential model which accounts explicitly for the size and charge of the salt ions is needed. Accounting for the excluded-volume effects of the ions via the osmotic-attraction potential given in Equation 7 is a first approximation. The multicomponent diffusion-interaction model presented here is expected to be of greater value in analysis of diffusion data for systems where the solute exhibits an equilibrium aggregate-size distribution wider

than that for lysozyme.

Conclusion

Dynamic light scattering has been used to study the aggregation of hen-egg-white lysozyme in aqueous solutions of ammonium sulfate at 25°C. The concentration dependence of lysozyme apparent diffusion coefficients was interpreted in the context of a two-body potential of mean force which includes repulsive hard-sphere and coulombic interactions and attractive dispersion and ion-osmotic interactions. Analysis of data at low pH for ionic strength to 1.0 M allowed regression of the effective monomer charge and Hamaker constant; these were then applied at higher pH and at higher ionic strengths. Minimal aggregation was calculated in all our solutions; no oligomers larger than trimers were present in significant concentration, even at the highest pH and ionic strength. The implication of these results for lysozyme precipitation and crystallization is that lysozyme exhibits a phase transition (which depends on pH, ionic strength, and salt identity) between soluble distributions of small aggregates and large macroscopic clusters, rather than a gradual increase in the aggregation state as ionic strength increases.

Acknowledgments

This work was supported by the Director, Office of Energy Research, Office of Basic Energy Sciences, Chemical Sciences Division of the U. S. Department of Energy under contract DE-AC03-76F00098. The authors are grateful to Mr. Sheldon Oppenheim (University of Iowa) for advice regarding chromatographic purification of lysozyme.

Nomenclature

a_1, a_i	monomer, aggregate activity, [mol/L]
A_{ij}	interaction parameter for *ij* pair, [L/mol]
B_{ij}	osmotic second virial coefficient for *ij* pair, [L/mol]
c_p	protein concentration, [mol/L]
$\overline{D}$	z-average apparent diffusion coefficient, [cm^2/sec]
D_0	zero-angle infinite-dilution diffusion coefficient, [cm^2/sec]
D_i	diffusion coefficient of an *i*-mer, [cm^2/sec]
$D_{i,0}$	infinite-dilution diffusion coefficient of an *i*-mer, [cm^2/sec]
$(dn/dc)_{T,p}$	refractive-index increment, [mL/g]
e	electron charge, = $1.602 \cdot 10^{-19}$ C
f_0	infinite dilution hydrodynamic friction factor
f_i	ellipsoidal-aggregate hydrodynamic friction factor
$F(r, \sigma_i')$	hydrodynamic interaction function for a solution of monodisperse spheres
$g_{ij}(r)$	pair-correlation function between *i*-mer and *j*-mer
$g^E(\tau)$	electric-field autocorrelation function
H	Hamaker constant, [J]
I	ionic strength of added salt, [mol/L]
k_B	Boltzmann's constant, = $1.38 \cdot 10^{-23}$ J/K
K	non-ideal indefinite isodesmic association equilibrium constant, [L/mol]

M, M_i	monomer, aggregate molecular weights, [g/mol]
n	refractive index
N_A	Avogadro's number, = $6.02 \cdot 10^{23}$ mol^{-1}
q	scattering-vector magnitude, = $(4\pi n / \lambda_{laser}) \cdot sin(\theta / 2)$, [cm^{-1}]
Q	second central moment of diffusion-coefficient distribution
r_0	infinite-dilution hydrodynamic radius, [Å]
r_x	crystallographic monomer unhydrated radius, [Å]
Δr	effective-sphere hydration/Stern layer thickness, [Å]
S_{ij}	multicomponent diffusion hydrodynamic interaction parameter for *ij* pair
T	absolute temperature, [°K]
W	potential of mean force, [J]
z_1, z_i	monomer, aggregate valence

<u>*Greek Symbols*</u>

α_x, β_x	crystallographic monomer ellipsoidal major, minor semiaxis, [Å]
α_i, β_i	effective ellipsoidal aggregate major, minor semiaxis, [Å]
γ_i	activity coefficient of *i*-mer
ε	effective-ellipsoid hydration/Stern layer thickness, [Å]
ε_0	dielectric permittivity of vacuum, = $8.854 \cdot 10^{-22}$ [C^2/N Å^2]
ε_r	dielectric constant of water, = 78.54 at 298K
ξ_i	ion-aggregate average radius, [Å]

η_0	salt-solution viscosity, [cp]
θ	scattering angle
κ	inverse Debye length, [$Å^{-1}$]
λ	slope of the normalized concentration-dependent diffusion coefficient
Λ_{ii}	multicomponent diffusion hydrodynamic interaction parameter for *ii* pair
$\bar{v}$	partial specific volume of lysozyme, = 0.703 mL/g
Π_{id}	ideal osmotic pressure, [$J \cdot Å^{-3}$]
ρ_s	total ion number density, [$Å^{-3}$]
σ_1, σ_i	monomer, aggregate unhydrated diameter, [Å]
σ_1', σ_i'	monomer, aggregate hydrated diameter, [Å]
$\overline{\sigma_{ion}}$	average ion diameter, [Å]
ϕ	protein volume fraction

References

Adams, E. T. Jr. and D. L. Filmer. 1966. Sedimentation equilibrium in reacting systems. IV. Verification of the theory. *Biochem.* 5(9):2971-2985.

Arakawa, T. and S. N. Timasheff. 1982. Preferential interactions of proteins with salts in concentrated solutions. *Biochem.* 21:6545-6552.

Asakura, S. and F. Oosawa. 1954. On interaction between two bodies immersed in a solution of macromolecules. *J. Chem. Phys.* 22:1255.

Banerjee, S. K., A. Pogolotti, and J. A. Rupley. 1975. Self-association of lysozyme. *J. Biol. Chem.* 250(20):8260-8266.

Batchelor, G. K. 1976. Brownian diffusion of particles with hydrodynamic interaction. *J. Fluid Mech.* 74(1):1-29.

Batchelor, G. K. 1983. Diffusion in a dilute polydisperse system of interacting spheres. *J. Fluid Mech.* 131:155-175.

Batchelor, G. K. 1982. Sedimentation in a dilute polydisperse system of interacting spheres. Part 1. General theory. *J. Fluid Mech.* 119:379-408.

Blake, C. C. F., L. N. Johnson, G. A. Mair, A. C. T. North, D. C. Phillips, and V. R. Sarma. 1967. *Proc. Roy. Soc. Ser. B, Biol. Sci.* 167:378-.

Boué, F., F. Lefaucheux, M. C. Robert, and I. Rosenman. 1993. Small angle neutron

scattering study of lysozyme solutions. *J. Cryst. Growth*. 133:246-254.

Bruzzesi, M. R., E. Chiancone, and E. Antonini. 1965. Association-dissociation properties of lysozyme. *Biochem.* 4(9):1796-1800.

Chiew, Y. C., D. E. Kuehner, H. W. Blanch, and J. M. Prausnitz. 1995. Molecular thermodynamics of salt-induced protein precipitation. *AIChE J.* 41(9):2150-2159.

Coen, C. J., H. W. Blanch, and J. M. Prausnitz. 1995. Salting out of aqueous proteins: phase equilibria and intermolecular potentials. *AIChE J.* 41(4):996-1004.

Corti, M. and V. Digiorgio. 1981. Quasi-elastic light scattering study of intermicellar interactions in aqueous sodium dodecyl sulfate solutions. *J. Phys. Chem.* 85:711-717.

Curtis, R. A., H. W. Blanch, and J. M. Prausnitz. 1997. Protein-protein and protein-salt interactions in aqueous protein solutions containing concentrated electrolyte. To appear in *Biotech. Bioeng.*

Deonier, R. C. and J. W. Williams. 1970. Self-association of muramidase (lysozyme) in solution at 25°C, pH 7.0, and $I = 0.20$. *Biochem.* 9(22):4260-4267.

Eberstein, W., Y. Georgalis, and W. Saenger. 1994. Molecular interactions in crystallizing lysozyme solutions studied by photon correlation spectroscopy. *J. Cryst. Growth.* 143:71-78.

Felderhof, B. U. 1978. Diffusion of interacting Brownian particles. *J. Phys. A: Math.*

Gen. 11(5):929-937.

Felderhof, B. U. 1977. Hydrodynamic interaction between two spheres. *Physica.* 89A:373-384.

George, A. and W. W. Wilson. 1994. Predicting protein crystallization from a dilute solution property. *Acta Cryst.* D50(361-365)

Hamaker, H. C. 1937. The London-van-der Waals attraction between spherical particles. *Physica A*. 4(10):1058-1072.

Israelachvili, J. N. 1992. Intermolecular and Surface Forces. 2nd ed. Academic Press, London.

Koppel, D. E. 1972. Analysis of macromolecular polydispersity in intensity correlation spectroscopy: The method of cumulants. *J. Chem. Phys.* 57(11):4814-4820.

Mahadevan, H. and C. K. Hall. 1992. Theory of precipitation of protein mixtures by nonionic polymer. *AIChE J.* 38(4):573-591.

Melander, W. and C. Horvath. 1977. Salt effects on hydrophobic interactions in precipitation and chromatography of proteins: An interpretation of lyotropic series. *Arch. Biochem. Biophys.* 183:200-215.

Mikol, V., E. Hirsch, and R. Giegé. 1990. Diagnostic of precipitant for biomacromolecule crystallization by quasi-elastic light scattering. *J. Mol. Biol.* 213:187-195.

Murphy, R. M., M. L. Yarmush, and C. K. Colton. 1991. Determining molecular weight

distribution of antigen-antibody complexes by quasi-elastic light scattering. *Biopol.* 31(11):1289-1295.

Muschol, M. and F. Rosenberger. 1995. Interactions in undersaturated and supersaturated lysozyme solutions: static and dynamic light scattering results. *J. Chem. Phys.* 103(24):10424-10432.

Muschol, M. and F. Rosenberger. 1996. Lack of evidence for prenucleation aggregate formation in lysozyme crystal growth solutions. *J. Cryst. Growth.* 167:738-747.

Nicoli, D. F. and G. B. Benedek. 1976. Study of thermal denaturation of lysozyme and other globular proteins by light-scattering spectroscopy. *Biopol.* 15:2421-2437.

Niimura, N., M. Ataka, Y. Minezaki, and T. Katsura. 1995a. Small-angle neutron scattering from lysozyme crystallization process. *Physica B.* 213&214:745-747.

Niimura, N., Y. Minezaki, M. Ataka, and T. Katsura. 1995b. Aggregation in supersaturated lysozyme solution studied by time-resolved small angle neutron scattering. *J. Cryst. Growth.* 154:136-144.

Niimura, N., Y. Minezaki, M. Ataka, and T. Katsura. 1994. Small angle neutron scattering from lysozyme in unsaturated solutions, to characterize the pre-crystallization process. *J. Cryst. Growth.* 137:671-675.

Norton, R. S. and A. Allerhand. 1977. Participation of tryptophan 62 in the self-association of hen egg white lysozyme. *J. Biol. Chem.* 252(5):1795-1798.

Provencher, S. W. 1982a. A constrained regularization method for inverting data represented by linear algebraic or integral equations. *Comput. Phys. Commun.* 27:213-227.

Provencher, S. W. 1982b. CONTIN: A general purpose constrained regularization program for inverting noisy linear algebraic and integral equations. *Comput. Phys. Commun.* 27:229-242.

Pusey, P. N. and Tough, R. J. A. 1985 Particle interactions. *In* Dynamic Light Scattering: Applications of Photon Correlation Spectroscopy. Pecora, R. Plenum Press, New York.

Riès-Kautt, M. and A. Ducruix. 1994. Crystallization of previously desalted lysozyme in the presence of sulfate ions. *Acta Cryst.* D50:366-369.

Rosenbaum, D., P. C. Zamora, and C. F. Zukoski. 1996. Phase behavior of small attractive colloidal particles. *Phys. Rev. Lett.* 76(1):150-153.

Roth, C. M., B. L. Neal, and A. M. Lenhoff. 1996. Van der Waals interactions involving proteins. *Biophys. J.* 70:977-987.

Rothstein, F. 1994. Protein Purification Process Engineering. Dekker, New York.

Rupley, J. A., L. Butler, M. Gerring, F. J. Hartdegen, and R. Pecoraro. 1967. *Proc. Nat. Acad. Sci. U.S.A.* 57:1088-.

Scopes, R. K. 1994. Protein Purification: Principles and Practice. Springer-Verlag, New

York.

Shen, C. L., G. L. Scott, F. Merchant, and R. M. Murphy. 1995. Light-scattering analysis of fibril growth from the amino-terminal fragment of β(1-28) of β-amyloid protein. *Biophys. J.* 65:2383-2395.

Skouri, M., M. Delsanti, J.-P. Munch, B. Lorber, and R. Giegé. 1991. Dynamic light scattering studies of the aggregation of lysozyme under crystallization conditions. *FEBS Letters.* 259(1-3):84-88.

Skouri, M., J.-P. Munch, B. Lorber, R. Giegé, and S. Candau. 1992. Interactions between lysozyme molecules under precrystallization conditions studied by light scattering. *J. Cryst. Growth.* 122:14-20.

Sophianopoulos, A. J. 1969. Association Sites of Lysozyme in Solution. *J. Biol. Chem.* 244(12):3188-3193.

Sophianopoulos, A. J., C. K. Rhodes, D. N. Holcomb, and K. E. Van Holde. 1962. Physical Studies of Lysozyme. I. Characterization. *J. Biol. Chem.* 237(4):1107-1112.

Sophianopoulos, A. J. and K. E. Van Holde. 1961. Evidence for Dimerization of Lysozyme in Alkaline Solution. *J. Biol. Chem.* 236(12):PC82-PC83.

Sophianopoulos, A. J. and K. E. Van Holde. 1964. Physical studies of muramidase (lysozyme) II. pH-dependent dimerization. *J. Biol. Chem.* 239(8):2516-2524.

Stepanek, P. 1993 Data analysis in dynamic light scattering. *In* Dynamic light scattering: The method and some applications. Wyn Brown. Clarendon Press, Oxford.

Tanford, C. and M. L. Wagner. 1954. Hydrogen ion equilibria of lysozyme. *J. Amer. Chem. Soc.* 76:3331-3336.

Tavares, F. W. and S. I. Sandler. 1997. Phase equilibrium for the mean-force potential of globular protein solutions. *AIChE J.* 43(1):218-231.

Thibault, F., J. Langowski, and R. Leberman. 1992. Optimizing protein crystallization by aggregate size distribution analysis using dynamic light scattering. *J. Cryst. Growth.* 122:50-59.

Verwey, E. J. W. and Overbeek, J. T. G. 1948. Theory of Stability of Lyophobic Colloids. Elsevier, Amsterdam.

Vlachy, V., H. W. Blanch, and J. M. Prausnitz. 1993. Liquid-liquid phase separations in aqueous solutions of globular proteins. *AIChE J.* 39(2):215-223.

Weast, R. C. 1981. Handbook of Chemistry and Physics. 62nd ed. CRC Press, Boca Raton.

Weiner, B. B. 1984 Particle sizing using photon correlation spectroscopy. *In* Modern Methods of Particle Size Analysis. Barth, H. John Wiley & Sons, New York. pp. 93-116.

Wills, P. R., L. W. Nichol, and R. J. Siezen. 1980. The indefinite self-association of

lysozyme: consideration of composition-dependent activity coefficients. *Biophys. Chem.* 11:71-82.

Zero, K. and Pecora, R. 1985 Dynamic depolarized light scattering. *In* Dynamic Light Scattering: Applications of Photon Correlation Spectroscopy. Pecora, R. Plenum Press, New York.

Appendix A: Calculation Scheme for Fitting Aggregation Equilibrium Constants

The activity coefficients of the i-mers, $\{\gamma_{ij}\}$, each depend on the concentrations of all aggregates, as described in Equation 14. As a result of this complex concentration dependence, an iterative method was required to determine K. At each solution condition, K was regressed under the constraint that, for each of the three protein solutions, the difference between the calculated and the experimental values of $\overline{D}$ was minimized while satisfying the total protein mass balance given in Equation 13. A flow diagram for this calculation procedure is shown in Figure A.1. In all cases, the mass balances were satisfied exactly, and in most cases the error between the calculated and experimental $\overline{D}$'s was less than 5%.

Calculation of the second virial coefficients, $\{B_{ij}\}$, and the multicomponent hydrodynamic interaction parameters, $\{S_{ij}\}$, required numerical integration to a large upper limit in distance, r, expressed in multiples of σ'_{ij}. In a trial calculation with the longest-ranged potential of mean force used in this work (corresponding to pH 4 and I = 0.05 M where screened coulombic repulsion is the dominant contribution to the overall potential), it was determined that the change in any of these integrated quantities that resulted from changing the upper limit of integration from $r/\sigma'_{ij} = 8$ to $r/\sigma'_{ij} = 9$ was less than 0.01%. Also, the maximum number of possible aggregates considered, N, determined how many virial coefficients needed to be calculated, $N(N+1)/2$. N is infinite for the indefinite isodesmic aggregation model. However, for the case where the highest value of

K was calculated, ionic strength 5.0 M and pH 7, the value of N, above which the value of K did not change by more than 0.01% with increasing N, was found to be 3, indicating that only small distributions of aggregates were present in the DLS samples.

Table 1: Diffusion coefficients, $\overline{D}$, of lysozyme in ammonium sulfate solutions, obtained from Zimm plots measured by dynamic light scattering at 25°C. All $\overline{D}$ values reflect extrapolation to zero scattering angle, and $\overline{D}$ values at zero volume fraction are infinite-dilution extrapolations, D_0. Here, **I** = ionic strength.

I [M]	pH	ϕ ($\cdot 10^3$)	$\overline{D}$ ($\cdot 10^6$) [cm²/sec]
0.05	4.25	0	1.298
		6.2	1.322
		12.3	1.345
		17.4	1.365
	4.9	0	1.277
		6.2	1.279
		12.9	1.283
		18.0	1.285
	6	0	1.370
		5.6	1.334
		11.4	1.300
		17.3	1.259
	6.86	0	1.267
		6.0	1.229
		12.0	1.171
		21.8	1.113
0.15	4.09	0	1.348
		5.8	1.305
		12.0	1.259
		18.5	1.210
	5.13	0	1.380
		5.8	1.305
		11.7	1.220
		18.1	1.142
	6	0	1.354
		5.5	1.279
		11.7	1.184
		18.3	1.097
	6.9	0	1.350
		4.9	1.289
		11.2	1.164
		17.5	1.102
0.30	4.15	0	1.306
		5.9	1.250
		12.0	1.176
		19.5	1.111
	5.03	0	1.342
		6.2	1.265
		13.5	1.169
		16.8	1.132
	5.97	0	1.309
		6.2	1.236
		13.4	1.132
		20.5	1.058
	0.30	0	1.305
		5.6	1.211
		12.2	1.123
		18.9	1.001
0.4	4.15	0	1.294
		6.3	1.230
		13.4	1.167
		20.4	1.092
0.50	4.02	0	1.332
		6.5	1.247
		13.3	1.152
		20.7	1.059
	5.22	0	1.378
		6.6	1.282
		14.5	1.141
		19.5	1.090
	6.00	0	1.336
		7.2	1.250
		15.5	1.111
		24.4	1.020
	6.9	0	1.337
		6.1	1.230
		12.9	1.086
		19.7	0.976
0.75	4.05	0	1.290
		7.4	1.198
		15.8	1.092
		24.2	0.990
1.0	3.97	0	1.340
		6.7	1.252
		13.2	1.153
		20.4	1.063
	5.03	0	1.355
		6.5	1.262
		13.5	1.159
		19.7	1.070
	6.15	0	1.361
		7.1	1.250
		14.7	1.129
		21.8	1.020
	6.89	0	1.276
		6.1	1.204
		13.2	1.085
		20.9	1.008
3.0	4.15	0	1.114
		6.8	0.995
		13.1	0.885
		19.6	0.770
	4.9	0	1.099
		6.6	0.986
		13.1	0.874
		19.3	0.765
	6.9	0	1.056
		6.9	0.954
		13.8	0.853
		22.1	0.730
4.0	4.15	0	1.053
		7.2	0.860
		9.4	0.799
		9.7	0.792
	4.95	0	1.020
		6.7	0.880
		9.8	0.818
		16.4	0.682
	6.1	0	0.998
		7.2	0.861
		10.2	0.803
		16.2	0.687
	6.9	0	0.980
		6.8	0.853
		13.4	0.729
		19.1	0.624
5.0	6.9	0	0.911
		6.0	0.724
		7.9	0.664
		8.3	0.650

Figure Captions

Figure 1: Dynamic Zimm plot for hen-egg-white lysozyme in ammonium sulfate: I = 4.0 M, pH = 6.1. Filled symbols represent DLS data; open symbols are extrapolations to zero angle or zero concentration. D_0 is given by the intersection of the (dotted) least-squares lines through the extrapolated values. Plotting constant $k = 10^9$.

Figure 2: Infinite-dilution hydrodynamic radii of lysozyme obtained from Stokes-Einstein relation. The average r_0 at pH 4 is 18Å (±0.5Å).

Figure 3: Normalized diffusion coefficients of lysozyme in ammonium sulfate solutions as a function of ϕ, the protein volume fraction. (a) Ionic-strength dependence at pH 4. (b) pH dependence at I = 1.0 M.

Figure 4: Effective ellipsoidal aggregate structure for a hydrated lysozyme dimer.

Figure 5: (a) Contributions to the potential of mean force between two protein monomers (i = 1) as a function of reduced distance for I = 0.05 M. The solid line represents the total potential of mean force. (b) Dependence of the potential of mean force on ionic strength. Parameters: z_1 = 10, H/k_BT = 5, σ_1 = 34.4 Å, Δr = 0.8 Å, $\overline{\sigma_{ion}}$ = 3.5 Å.

Figure 6: Fitting effective monomer charge and Hamaker constant at pH 4 to the experimental data in Figure 3(*a*). The common intersection of these curves gives the ionic-strength-independent values of H/k_BT and z_1.

Figure 7: Dependence of parameters H/k_BT and z_1 on the value of Δr, the thickness of the hydration/Stern layer, for lysozyme at pH 4. In this work, the value of Δr = 0.8 Å, giving H/k_BT = 7.6 and z_1 = 5.3.

Figure A.1: Flow diagram for calculating aggregation equilibrium constants from diffusion data.

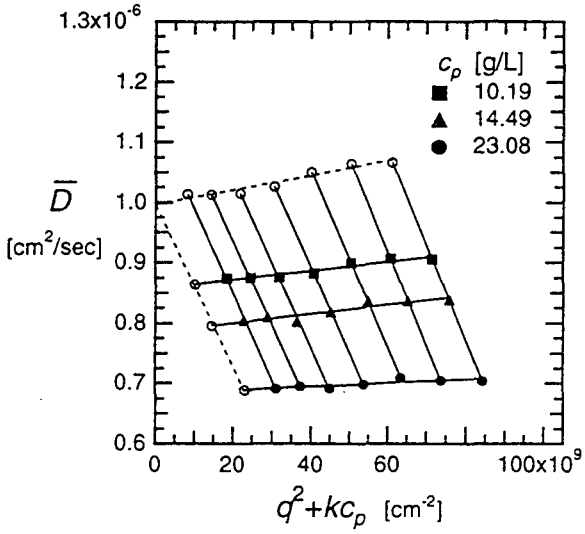

Kuehner, *et al.*, Figure 1

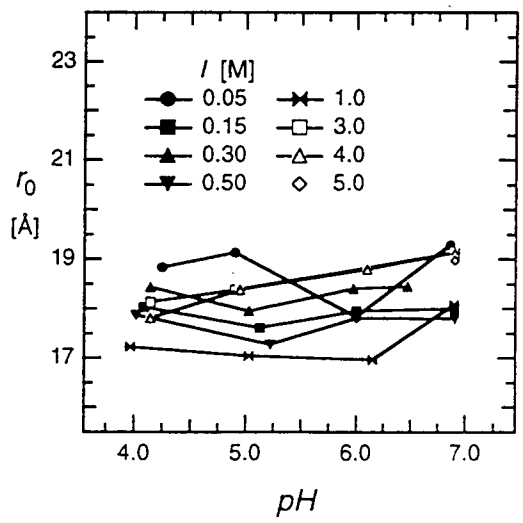

Kuehner, *et al.*, Figure 2

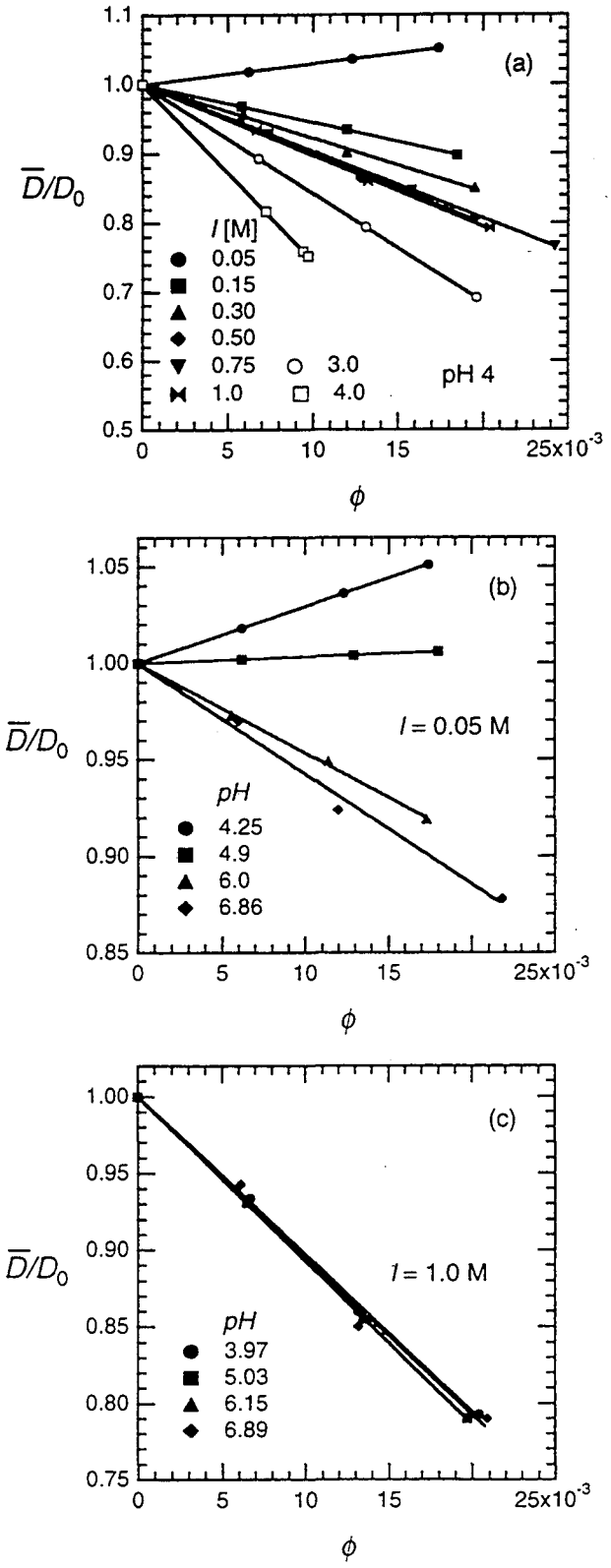

Kuehner, *et al.*, Figure 3

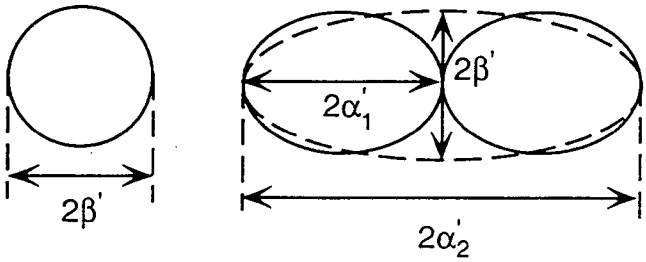

Kuehner, *et al.*, Figure 4

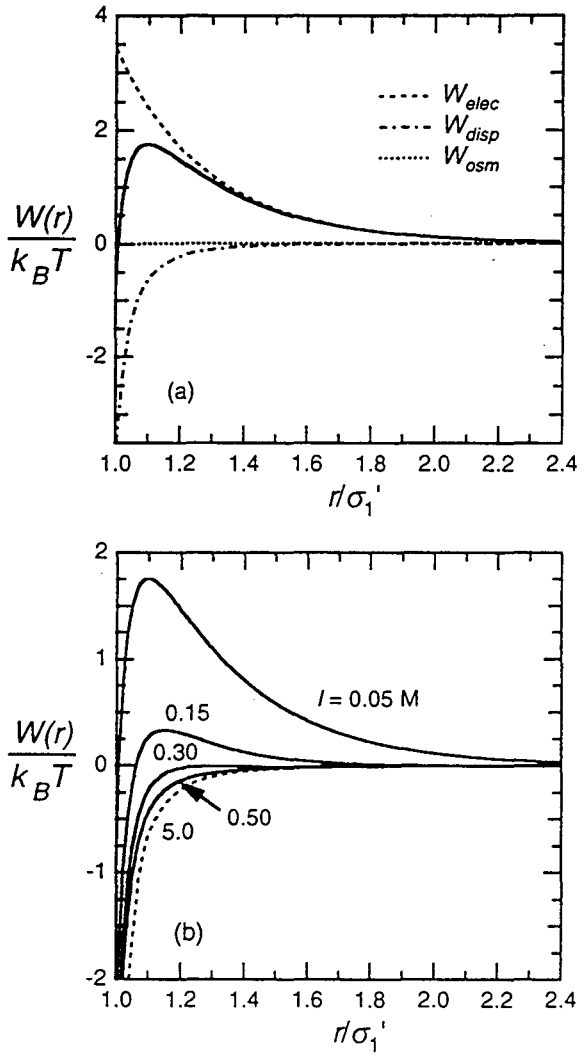

Kuehner, *et al.*, Figure 5

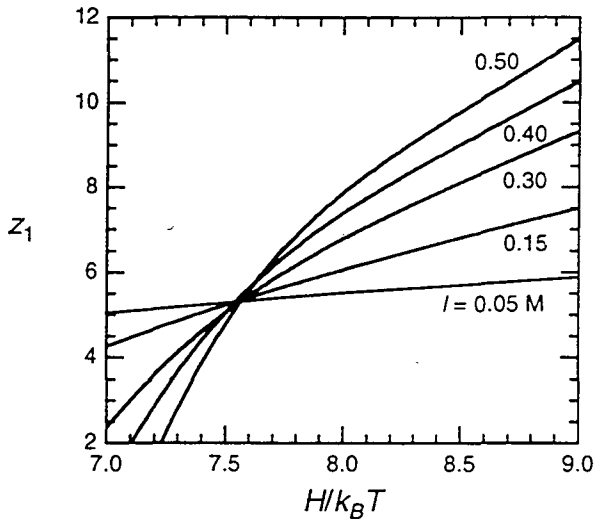

Kuehner, *et al.*, Figure 6

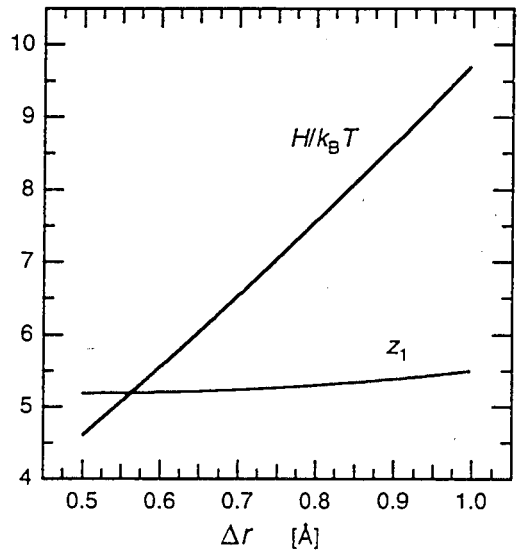

Kuehner, *et al.*, Figure 7

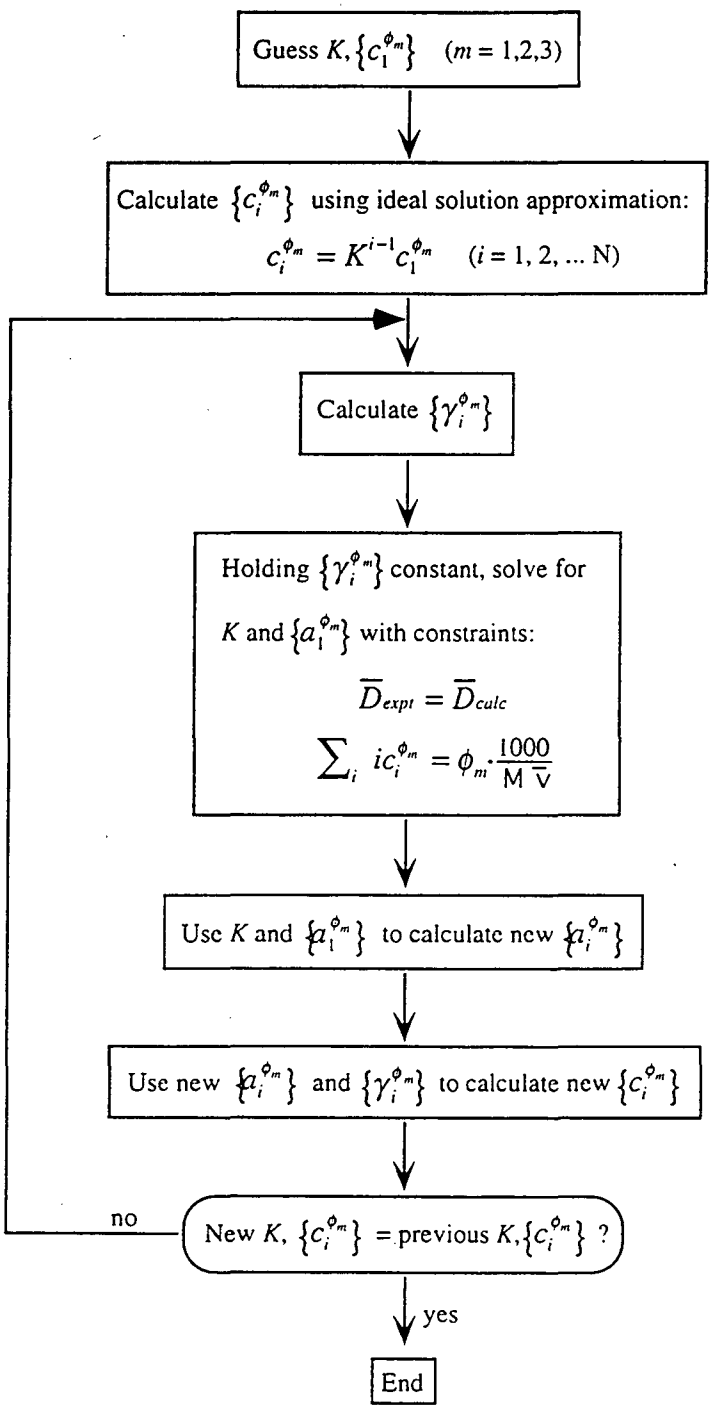

Kuehner, *et al.*, Figure A.1

Ernest Orlando Lawrence Berkeley National Laboratory
One Cyclotron Road | Berkeley, California 94720

Prepared for the U.S. Department of Energy under Contract No. DE-AC03-76SF00098